Chapter 12

Effects of Different Laser Pulse Regimes (Nanosecond, Picosecond and Femtosecond) on the Ablation of Materials for Production of Nanoparticles in Liquid Solution

Abubaker Hassan Hamad

Additional information is available at the end of the chapter

http://dx.doi.org/10.5772/63892

Abstract

Ultra-short laser pulse interaction with materials has received much attention from researchers in micro- and nanomachining, especially for the generation of nanoparticles in liquid environments, because of the straightforward method and direct application for organic solvents. In addition, the colloidal nanoparticles produced by laser ablation have very high purity—they are free from surfactants and reaction products or by-products. In this chapter, nanosecond, picosecond and femtosecond laser pulse durations are compared in laser material processing. Due to the unique properties of the short and ultra-short laser pulse durations in material processing, they are more apparent in the production of precision material processing and generation of nanoparticles in liquid environments.

Keywords: lasers, laser ablation, nanoparticles, pulse duration, nanosecond lasers, picosecond lasers, femtosecond lasers

1. Introduction

Different laser pulse regimes (nanosecond, picosecond and femtosecond) were used not only to generate nanoparticles but also to manipulate them. Different laser wavelengths were selected to reduce the size of the nanoparticles and change their morphology. The study in this filed focuses on using different laser types and parameters to generate and manipulate of micro- and nanomaterials. Researchers have used different types of lasers not only to produce new materials

but also for precise micro- and nanomachining. Generating lasers with short and ultra-short pulse duration leads to high-precision laser processing. Lasers with pulse durations in the femtosecond to picosecond range demonstrate a significant development in quality for different materials in comparison with nanosecond or longer laser pulses [1]. In addition, using pulsed lasers to produce nanoparticles in liquid environments is a promising alternative to chemical methods for the production of totally ligand-free colloidal nanoparticles [2].

In general, for laser material processing, two different laser pulse duration regimes are used: long pulse duration, such as nanosecond pulse duration, which generates quite a significant heat-affected zone in the material because "the pulse duration is longer than the thermalisation time of most metals" [3]. This type of laser is suitable for removing materials or ablation. Short pulse duration (picosecond laser) and ultra-short pulse duration (femtosecond laser) yield better results, suited to the production of high-precision micro- and nanomachining. Typical laser pulse durations for precise laser material processing are 10 ps or less. It has been shown that suitable laser pulse durations for the micromachining of copper and stainless steel are in the range of 10–100 ps [3].

However, there is little evidence that researchers have approached the issue of lasers in nanotechnology in terms of precise and controllable ablation and their ability to generate nanoparticles from different materials. Consequently, the aim of this chapter is to provide an overview of how different laser pulses can be used in laser-material interaction and the production of nanoparticles.

Two important parameters used to describe lasers are their pulse duration (width) and pulse repetition rate (PRR). As shown in **Figure 1a**, laser pulse duration can also be described as full-width at half of the maximum (FWHM) amplitude of the laser pulse. Pulse repetition rate or pulse repetition frequency refers to the number of pulses emitted per second. For 1 kHz of PRR, the time period *T* would be 0.001 s (see **Figure 1b**).

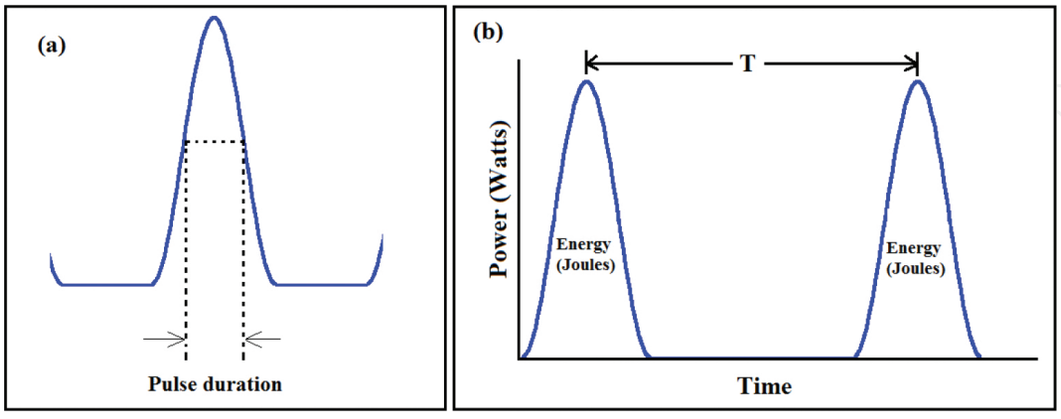

Figure 1. Pulse width or pulse duration (a) and pulse repetition rate (b) of a laser.

Two further parameters of pulsed lasers, which are especially relevant for ultrafast lasers, are the laser's peak power (P_{peak}), which is equal to the laser pulse energy divided by laser pulse

http://dx.doi.org/10.5772/63892

duration ($P_{peak} = E_p/\tau$) and the average laser power, which is equivalent to the laser pulse energy multiplied by the pulse repetition rate ($P_{ave.} = E_p \times PRR$) [4].

In this chapter, the author shows the effects of different laser pulse interactions (nanosecond, picosecond and femtosecond lasers) with materials and the ablation of nanoparticles in a liquid environment in terms of their size, size distribution, morphology and production rate (productivity).

2. Pulsed laser ablation

Ultra-short laser pulse duration in the range of femtosecond laser pulses and a few picoseconds can be used to produce high-quality and precise material processing. Ultra-short pulse duration can only interact with electrons but longer pulse duration interacts with lattice. It is worth mentioning that during the interaction of an ultra-short laser pulse with materials, heat conduction is limited [5]. As a result of this, the material will be ablated within a spatial or well-defined area with minimised mechanical and thermal damage of the ablated area on the target. In contrast, longer (nanosecond) pulse duration irradiation on the materials leads to continuously heating the target material. The laser pulse energy will then be spread by heat conduction to an area outside the laser spot size, causing the irradiated target to boil and evaporate. Boiling and evaporation of the target material leads to the production of an uncontrollable melt layer [6]. In the case of nanosecond laser pulse duration, this problem may be caused by imprecise machining or marking.

There is existing research on laser-material interaction [6–8]; however, these show how differently pulsed lasers can be used for material processing, especially in nanotechnology. Furthermore, there are relevant findings concerning laser ablation of nanoparticles in liquid environments [9–12], and they are somewhat showing the effects of different laser pulse durations on the ablation of nanoparticles. Even most previous research on laser-material interaction and laser-generated nanoparticles tends to highlight laser beam parameters and experimental setups to produce small and well-distributed nanoparticles and to precision material processing, there is little emphasis on the optimal laser parameters to apply in laser material processing. Moreover, little attention has been given to the conceptualisation of the structure and phase of the nanoparticles produced by laser ablation in a liquid solution. Consequently, an understanding of the optimal pulse regime for these applications is critical in order to support and enhance the performance of laser material processing in nanotechnology.

3. Laser-material interaction at different laser pulse durations

Laser ablation of the materials starts with photon absorption, followed by the heating and photoionisation of the subjected area on the target by the laser beam. Subsequently, the ablated materials released from the target surface as solid fragments, vapours, liquid drops or as an expanding plasma plume. The amount of ablated material and phase depends on the absor-

bed energy by the target material [13]. After laser-material interaction with short pulses and low intensity, due to the inverse Bremsstrahlung, the laser beam energy will be absorbed by free electrons from the material followed by thermalisation within the electrons, and energy transfer to the lattice. Finally, energy will be lost due to electron heat transfer to the target material. The energy transfer from the laser beam to the target material can be described using 1D and 2D diffusion models when this is considered rapid thermalisation in the electron subsystem and if both lattice and electron subsystems are characterised by their temperatures (T_i lattice temperature and T_e electron temperature) [5]:

$$C_e \frac{\partial T_e}{\partial t} = -\frac{\partial Q(z)}{\partial z} - \gamma\left(T_e - T_i\right) + S \tag{1}$$

$$C_i \frac{\partial T_i}{\partial t} = \gamma\left(T_e - T_i\right) \tag{2}$$

$$Q(z) = -k_e\left(\frac{\partial T_e}{\partial z}\right) \tag{3}$$

$$S = I(t)\, A\alpha\, e^{-\alpha z} \tag{4}$$

where $Q(z)$ is the heat flux along the z-axis perpendicular to the target material surface, S is the laser heating source, $I(t)$ is the laser intensity as a function of time, A is the surface transmissivity ($A = 1 - R$), R is the reflectivity of the target material, α is the absorption coefficient of the target material, C_e is the heat capacity of the electrons per unit volume, C_i is the lattice heat capacity per unit volume, γ is the parameter characterising the electron-lattice coupling, and k_e is the thermal conductivity of the electrons. Two non-linear differential Eqs. (1) and (2) are used to model the cooling dynamics for T_e and T_i, which account for the electron-phonon coupling and thermal conductivity of the sample material [14]. In addition, these equations can be used to model the time evolution of the electron and lattice temperatures, T_e and T_i [15]. Eqs. (1)–(4) can be written as:

$$C_e \frac{\partial T_e}{\partial t} = k_e\left(\frac{\partial^2 T_e}{\partial z^2}\right) - C_i \frac{\partial T_i}{\partial t} + I(t)\, A\alpha e^{-\alpha z} \tag{5}$$

The lattice heat capacity (C_i) is considerably higher than the electronic heat capacity (C_e); in this case, the electrons have a very high temperature. When the Fermi energy is higher than the electron energy, the non-equilibrium thermal conductivity and heat capacity of the electron can be written as $k_e = k_o\,(T_i).T_e/T_i$ and $C_e = C'_e T_e$, respectively, where $k_o(T_i)$ is the conventional equilibrium thermal conductivity of a material and C'_e is a constant. In Eq. (5), a thermal

http://dx.doi.org/10.5772/63892

conductivity in the lattice subsystem (phonon component) is neglected, and it has three characteristic timescales; τ_e is the electron cooling time ($\tau_e = C_e/\gamma$), τ_i is the lattice heating time ($\tau_e << \tau_i$) ($\tau_i = C_i/\gamma$), and τ_L is the laser pulse duration. In laser-material interaction, these parameters define three different interaction regimes: nanosecond, picosecond and femtosecond [5].

Zimmer [16] proposed a model for the analytical solution of the laser-induced temperature distribution across internal solid-liquid interfaces (see **Figure 2a**). It was shown that high solid surface temperature can be obtained with short laser pulse durations, sufficient interface absorption and high absorption liquids. As shown in **Figure 2b**, in the case of using a nanosecond laser (20 ns), the temperature of the liquid environment is quite higher than that of the transparent solid material.

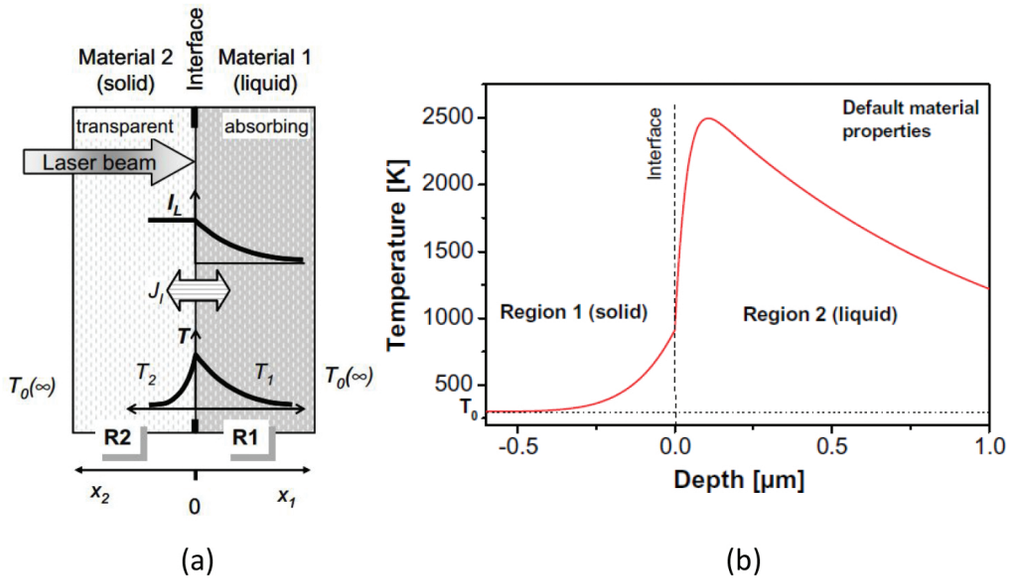

Figure 2. Diagram showing laser heating of a solid-liquid interface. I_L is the laser absorption, T is the temperature distribution in both materials, and J_I is the heat conduction across the interface [16].

3.1. Nanosecond laser

It was shown that the laser pulse duration has an effect on both the material ablation thresholds and penetration depths. Long pulse duration or increasing laser pulse duration increases the threshold fluence and decreases the effective energy penetration depth [1]. Low-intensity long laser pulse interaction with a target material firstly heats the surface of the target due to the absorbed energy, which leads to melting and vaporisation. It should be noted that vaporisation of the target requires much more energy than melting. "In case of low laser intensities the created vapour remains transparent for the laser radiation". The electron and lattice (ion) temperatures are equal ($T_e = T_i = T$) [6]. In other words, if the laser pulse duration is long in comparison with the electron-phonon energy-transfer time ($\tau_L >> \tau_i$), the electrons and lattice temperatures will remain at the same thermal equilibrium point ($T_e = T_i = T$) [5, 17]; as such, Eq. (5) reduces to the heat equation:

$$C_i \frac{\partial T}{\partial t} = k_o \left(\frac{\partial^2 T}{\partial z^2} \right) + I_\alpha \alpha e^{-\alpha z} \tag{6}$$

In nanosecond laser beam interaction with material, the surface of the target material will be heated to melting point and then to vaporisation temperature. During the laser-material interaction, energy will be lost as heat conduction into the target material; the heat penetration depth (l) is given by $l \sim (D_t)^{1/2}$, where D is the heat diffusion coefficient and is given by ($D = k_o/C_i$). It can be noted that for this regime of lasers, the condition $D\tau_L\alpha^2 >> 1$ is fulfilled, for example the thermal penetration depth is quite larger than the optical penetration depth [18]. The energy deposited in the target material per unit mass is given by $E_m \sim I_\alpha t/pl$; at a specific time ($t = t_{th}$), this energy becomes higher than the specific heat of evaporation Ω, at which point considerable evaporation will occur. When $E_m \sim \Omega$, the results are $t_{th} \sim D(\Omega\varrho/I)^2$. Consequently, for strong evaporation conditions, $E_m > \Omega$ or $\tau_L > f_{th}$ can be written for laser intensity as [5, 6]:

$$I > I_{th} \sim \frac{\rho \Omega D^{1/2}}{\tau_L^{1/2}} \tag{7}$$

and for laser fluence as:

$$F > F_{th} \sim \rho \Omega D^{1/2} \times \tau_L^{1/2} \tag{8}$$

The threshold laser fluence increases as $\tau_L^{1/2}$. In nanosecond laser ablation regimes, there is enough time for thermal waves to propagate into the target material and to create a relatively large layer of melted material target [5, 6]. Nanosecond laser pulses can ablate the target materials even at low laser intensities in both the vapour and liquid phases, so a recoil pressure that expels the liquid will be created due to the vaporisation process [6]. Evaporation occurrence makes challenge to precise laser processing with nanosecond laser pulses [18].

At long laser pulse duration, interaction with materials usually fulfils the condition $L_{th} >> \alpha^{-1}$, L_{th} being the heat-penetration depth which is given by $L_{th} \approx (2D\tau_p)^{1/2}$, where $D = k/\rho c$, D is the heat-diffusion coefficient. So, long laser pulse duration creates sufficient time for thermal waves to propagate within the target material, and the absorbed energy will be stored in a layer with a thickness of about L_{th}. In this case, the target material needs much more energy to vaporise than to melt; in other words, evaporation will occur, while the energy absorbed per unit volume into the vaporised layer becomes higher than the latent heat of evaporation per unit volume, namely [19].

$$\Delta z_\upsilon \approx \frac{A\left(F_L - F_{th}\right)}{\rho L_\upsilon} \tag{9}$$

http://dx.doi.org/10.5772/63892

where F_{th} is the laser fluence threshold which represents the minimum energy above which appreciable evaporation occurs from liquid metals. This figure is approximately given by the energy required to melt a surface layer of the target material of the order of L_{th} [19]:

$$F_{th} \approx \frac{\rho c \Delta T_m L_{th}}{A} \tag{10}$$

where $\Delta T_m = T_m - T_o$ and T_m and T_o are the melting and initial target temperature, respectively.

3.2. Picosecond laser

At low-intensity, short laser pulse interactions with a target material, due to the inverse Bremsstrahlung most of the laser energy will be absorbed by the free electrons of the target. This result can be described by the difference between the electron and lattice temperatures ($T_e > T_i$) in a transient nano-equilibrium state. In spite of a small energy exchange between the lattice and the electron heat conduction, the electrons are cooled [6]. For picosecond laser ablation, time t is much greater than τ_e ($t >> \tau_e$), which is equivalent to $C_e T_e / t << \gamma T_e$. In addition, when the condition $\tau_e << \tau_L << \tau_i$ is fulfilled, Eq. (1) becomes quasi-stationary for the electron temperature [5]. In other words, when the laser pulse duration is shorter than the electron-phonon energy-transfer time, then the electron and lattice have different temperatures, meaning that they will be in a non-thermal equilibrium state. In this case, Eq. (5) becomes the following equations [5, 17]:

$$k_e \left(\frac{\partial^2 T_e}{\partial z^2} \right) - \gamma \left(T_e - T_i \right) + I_\alpha \alpha e^{(-\alpha z)} = 0 \tag{11}$$

$$T_i = T_o + \frac{1}{\tau_i} \int_0^t e^{\left(\frac{t-\theta}{\tau_i} \right)} T_e(\theta) d\theta \tag{12}$$

This method represents the lattice temperature in integral from. The above equations describe heating of metal targets by the laser pulses when the laser pulse duration $\tau_L >> \tau_e$. By neglecting T_o and when $t << \tau_i$, because of the quasi-stationary character of the electron temperature, Eq. (12) can be reduced as follows [5, 18]:

$$T_i \simeq T_e \left(1 - e^{\left(-\frac{t}{\tau_i} \right)} \right) \simeq \left(\frac{t}{\tau_i} \right) T_e \tag{13}$$

It can be noted from the last equation that during picosecond laser ablation, the lattice temperature remains notably lower than the electron temperature, and thus, the lattice temperature in Eq. (11) can be neglected.

When $k_e T_e \alpha^2 \ll \gamma T_e$, from Eqs. (11) and (13), it can be concluded that the electron cooling is due to an exchange of energy with the lattice of the material target. Finally, both the lattice and electron temperature at the end of the laser pulse can be expressed by the following equation [5]:

$$T_e \simeq \frac{I_\alpha \alpha}{\gamma} e^{(-\alpha z)} \text{ and } T_i \simeq \frac{F_\alpha \alpha}{C_i} e^{(-\alpha z)} \tag{14}$$

It can be noted that when the condition $\tau_e \ll \tau_L$ is fulfilled, at the end of the pulse, both lattice temperature and attainable lattice temperature are approximately equal.

3.3. Femtosecond laser

For femtosecond lasers, if the laser pulse duration τ_L is assumed to be shorter than the electron cooling time τ_e. ($\tau_L \ll \tau_e$.) and when $t \ll \tau_e$, it is equivalent to $C_e T_e / t \gg \gamma T_e$. In this case, the electron-lattice coupling can be neglected and Eq. (1) can be solved easily. When $D_e \tau_L < \alpha^2$ (where $D_e = k_e / C_e$ is the electron thermal diffusivity) is fulfilled, to simplify the solution of the equation, the electron heat conduction term can be neglected. Thus, Eq. (1) can be written as [5]:

$$C_e^{'} \left(\frac{\partial T_e^2}{\partial t^2} \right) = 2 I_\alpha \alpha e^{(-\alpha z)} \tag{15}$$

which gives

$$T_e(t) = \left(T_o^2 + \frac{2 I_\alpha \alpha}{C_e^{`}} t e^{(-\alpha z)} \right)^{1/2} \tag{16}$$

where $I(t) = I_o$ is assumed constant, and $I_\alpha = I_o A$, and $T_o = T_e(0)$ refer to the initial temperature.

It has been shown that heat conduction of the target material can be neglected at the very short timescales of picosecond and femtosecond laser pulse durations; thus the target temperature at the end of the pulse within the target material can be given by [19].

$$T(z, \tau_L) \approx \left(\frac{\alpha A F_\alpha}{\rho c} \right) e^{(-\alpha z)} \tag{17}$$

where $F_\alpha = I_o \tau_L$ is the laser pulse fluence, and τ_L is the laser pulse duration.

http://dx.doi.org/10.5772/63892

The evolution of the electron temperature (T_e) and lattice temperatures (T_i) after the laser pulse is described by Eq. (5) with S = 0. In addition, the electron temperature and lattice temperature initial conditions are given by Eq. (17) and $T_i = T_o$. Due to the energy transfer to the lattice and heat conduction of the bulk material, the electrons are rapidly cooled after the laser pulse. Since the electron cooling time is quite short, then Eq. (2) can be written as $T_i \simeq T_e(\tau_L)t/\tau_i$. It should be noted that the initial lattice temperature is neglected here. On the other hand, the attainable lattice temperature is determined by the average cooling time of the electrons $\tau_e^{\alpha} = C_e^{`} T_e(\tau_L)/2\gamma$ and is given by the following equation [5]:

$$T_i \simeq T_e^2(\tau_L)\frac{C_e^{`}}{2C_i} \simeq \frac{F_\alpha \alpha}{C_i} e^{(-\alpha z)} \tag{18}$$

Fann et al. [20] and Wang et al. [14] have shown that the time scale for significant energy transfer and fast electron cooling is about 1 ps. In the case of $C_i T_i >> \varrho\Omega$, where ϱ is the density and Ω is the specific heat of evaporation per unit mass, considerable evaporation will occur. From Eq. (18), the conditions for strong evaporation can be given in the form:

$$F_\alpha \geq F_{th}\ e^{(\alpha z)} \tag{19}$$

where $F_{th} = \varrho\Omega/\alpha$ is the threshold fluence laser evaporation by femtosecond laser pulses. Then, the ablation depth per laser pulse (or ablation rate) L can be written as [5, 21]:

$$L \simeq \alpha^{-1} \ln\left(\frac{F_\alpha}{F_{th}}\right) \tag{20}$$

The logarithmic dependence of the ablation depth on the laser pulse fluence is well known for the laser ablation of organic polymers and metal targets with femtosecond pulse duration [5].

It can be noted that Eqs. (14) and (18) give the same expressions for the lattice temperature in both picosecond and femtosecond laser regimes. Therefore, the condition for strong evaporation given by (19), the fluence threshold and the ablation depth per pulse given by (20) remain unchanged [5, 18]. Thus, in the picosecond laser range, it is possible that logarithmic dependence of the ablation depth on the fluence exists. Here, electron heat conduction inside the target material is neglected. In this case, laser ablation is accompanied by the electron heat conduction and production of a melted area in the target material. Even evaporation can be considered as a direct solid-vapour transition process, whereby the existence of a liquid phase in the target material reduces the precision of laser material processing. Femtosecond laser ablation effects a direct solid-vapour transition due to the short timescales in this laser regime; as a result of this, the lattice is heated on a picosecond timescale, leading to the production of vapour and plasma phases followed by a rapid expansion in vacuum. Here, in a first approx-

imation, thermal conduction into the target material can be neglected during all of the aforementioned processes. Due to the advanced properties of picosecond laser ablation, highly precise and pure laser material processing can be achieved, as has been experimentally demonstrated by Chichkov et al. [5].

4. Comparison of different pulse durations for the ablation of materials and production of nanoparticles

A comparison of the characteristics of nano-, pico- and femtosecond lasers produced nanoparticles and materials processing have been studied [5, 22]. Even the comparison is not a like-for-like; the experimental work should be assumed as a fare comparison between these types of commercial lasers operating at their usual operating conditions [22]. Nanosecond laser ablation of materials occurs due to "melt expulsion driven by the vapour pressure and the recoil pressure of light". The melted material will solidify again because of the instability of this process, in which the fluid phase dynamics and the driving vapour conditions are very complex. As a result of this, the ablated area on the surface of the material target is not precise and uniform in comparison with that produced by a femtosecond laser (see **Figure 3**). Furthermore, nanosecond laser ablation creates a heat-affected zone (HAZ) [4]. It was shown that the HAZ of Al sample for the nanosecond laser ablation was about 40 mm wide, whereas for the femtosecond laser there was not observable because it was <2 mm wide [23].

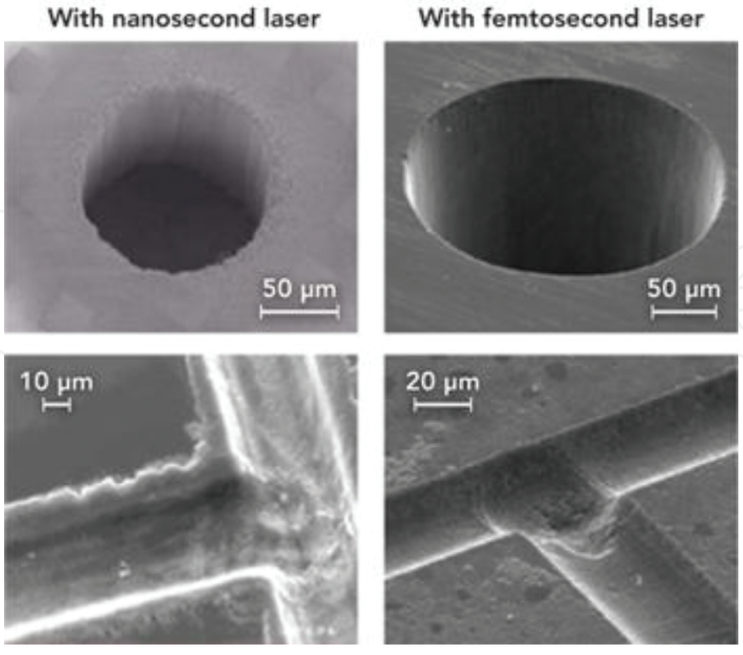

Figure 3. Laser material processing of a glass target by nanosecond laser (left) and femtosecond laser (right) ablation [4].

http://dx.doi.org/10.5772/63892

In the case of short (picosecond laser) and ultra-short laser pulses (femtosecond lasers), their pulse duration (τ) is considerably shorter than the timescale required for energy transfer between the lattice and the free electrons of the material target. As a result of this, very high temperatures and pressures are produced at a very shallow depth in the range of microns. Conversely, irradiated material is heated rapidly by pulsed laser and directly reaches the vapour phase with high kinetic energy without passing through the melting point temperature due to the absorbed energy. In other words, the material ablation will take place by vaporisation without producing a recast layer on the ablated area. As shown in **Figure 3**, the ablated area is very precise and smooth without forming any observable heat-affected zone (HAZ) [4]. The target materials with a high thermal conductivity are very important for the femtosecond laser ablation process because of the stable properties and chemical composition of the area ablated with femtosecond laser ablation [24].

For ultrafast lasers, laser beam energy deposition happens on a timescale that is quite short in comparison with atomic relaxation processes. After the laser energy is absorbed by the electrons, cold ions will be produced, leading to the occurrence of thermalisation at the end of the laser pulse. In addition, the femtosecond laser intensity is quite high and is sufficient to drive highly non-linear absorption processes in the target materials which the laser wavelength cannot absorb. At these high intensities, multi-photon ionisation becomes considerably strong [4]. Because of the very high flux of the femtosecond laser photons, several photons collide and become bound electrons; this is multi-photon ionisation. When the amount of total photon energies absorbed is higher than the ionisation potential, the bound electrons will absorb several photons. As a result, the bound electrons become free from the valence band. The multi-photon ionisation process is higher at very high laser intensities. When the laser intensity (photon flux) is above 10^{13} W/cm^2, multi-photon ionisation becomes very strong and seed electrons are not required to initialise ionisation in high-energy band gap materials or wide band gap materials (see **Figure 4a**) [4].

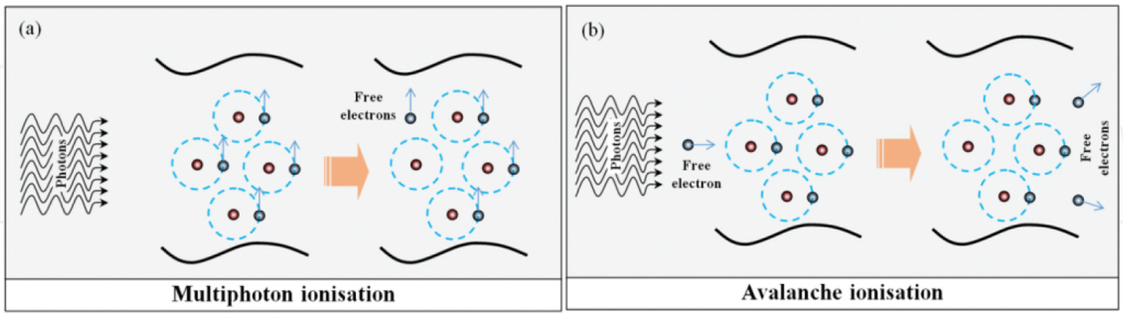

Figure 4. Non-linear ionisation processes of multi-photon absorption (a) and avalanche ionisation (b).

If the kinetic energy of the free electron is very high, some of the energy might be transferred to a bound electron in the target material by collision, thus overcoming the ionisation potential and generating two free electrons; this process is known as (collisional) impact ionisation. Thus, more free electrons will be produced from the bound electrons after the free electrons have absorbed photons. This is called avalanche ionisation, in which free electron

density exponentially increases. It is worth mentioning that avalanche ionisation is highly dependent upon free electron density. Energy loss by phonon emission and energy gain by inverse Bremsstrahlung competition indicate the efficiency of this process. It is responsible for the high-energy gap transition materials at laser intensities below 10^{12} W/cm^2 (see **Figure 4b**) [4]. For femtosecond lasers, avalanche ionisation plays an essential role in the optical breakdown. Briefly, avalanche ionisation produces a macroscopic breakdown of the target materials and multi-photon ionisation produces seed electrons at a critical density of about 10^{20} cm^{-3} [25].

The amount of material removed during laser ablation depends on the amount of energy absorbed by the bulk material target. The dissipation of the absorbed laser energy will usually occur after the laser pulse duration. There are two major mechanisms to explain material removal by laser ablation: thermal vaporisation, where the local temperature increases to above the vaporisation point due to the electron-phonon collisions, and the occurrence of a Coulomb explosion, where the bulk materials release the excited electrons and produce a relatively strong electric field which revokes the ions inside the impact area [4, 26]. According to these mechanisms, femtosecond laser material removal can be classified in two ways: the first is "strong ablation dominated by thermal vaporisation at intensities significantly higher than the ablation threshold" and the second is "gentle ablation governed by the Coulomb explosion near the ablation threshold" [4]. As shown in **Figure 5**, the long-pulse lasers have more heat-affected zones and shock waves in comparison with the shorter picosecond and femtosecond lasers. The main differences between them are due to the mechanism or the basic principles of laser-induced target material removal processes [27].

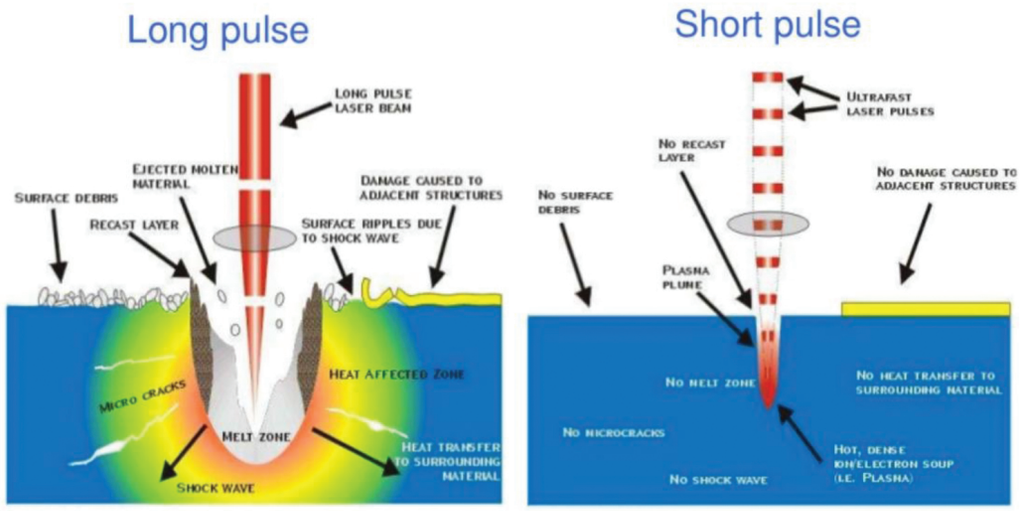

Figure 5. Long-pulse and ultrafast-pulse laser interaction with target material [27].

Laser pulse duration is an important parameter in the laser ablation process. There are quite large differences between the long pulse duration (nanosecond laser) and ultra-short laser pulse duration (femtosecond laser) for the ablation of materials [26]. As shown in **Figure 6**, during nanosecond laser ablation, plasma will be produced during the laser pulse, but during

http://dx.doi.org/10.5772/63892

femtosecond laser ablation, it will be produced after the laser pulse has ended. During nanosecond laser ablation, plasma is a part of the pulse duration, so the pulse serves to reheat the plasma. This leads to higher persistence of the plasma for nanosecond laser ablation than for femtosecond laser ablation [26].

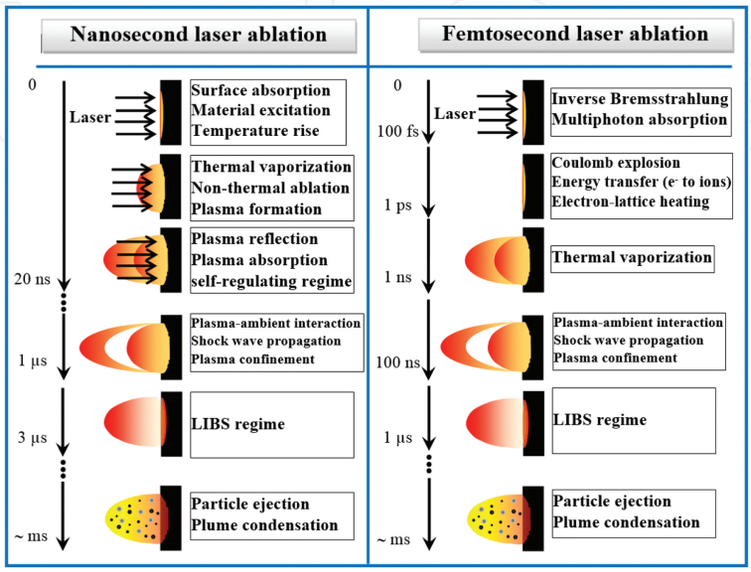

Figure 6. Approximate timescale comparison of pulsed laser energy absorption and ablation, along with the various processes, for nanosecond laser (10 ns) and femtosecond laser (50 fs) ablation in an ambient gas.

As shown in the schematic diagram in **Figure 7**, Lescoute et al. [28] showed that during subpicosecond laser ablation three phases occur behind the shock: liquid, vapour and plasma. The shock waves produced can compress the solid target material. The plasma plume effect is more predominant in picosecond laser ablation than in femtosecond laser ablation [22]. In general, laser-plasma interaction during laser-material ablation is strongly dependent on laser wavelength and the excitation wavelength is a very important parameter in nanosecond laser ablation, as in femtosecond laser ablation. The production of nanoparticles through plasma plume condensation occurs in the microsecond-millisecond timescales.

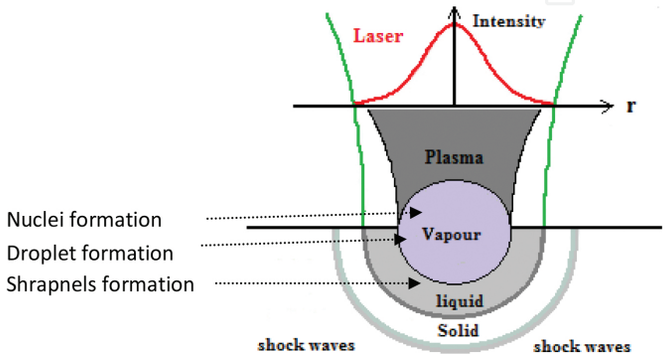

Figure 7. Schematic diagram of ablated matter depicted in an ultra-short, that is subpicosecond, laser-material interaction.

Another advantage of the femtosecond laser is its short timescale which prevents the material target from being heated; this leads to a reduction in the thermal effects in comparison with the nanosecond laser ablation. The duration of the energy transfer process from electron to ion (τ_{ei}) is approximately 1–10 s of a picosecond; this is in the same order as the heat conduction time (τ_{heat}). In an ideal femtosecond laser ablation case, this is considerably longer than the laser pulse duration (t_p). ($\tau_{ei} \sim \tau_{heat} >> t_p$) [26]. This will depend on the type of material sample.

Femtosecond laser energy transfer in the material for ablation will occur through energy absorption by electrons, leading to ionisation and then redistribution of the laser energy to the lattice. Ionisation is either produced by multi-photon ionisation or collisional impact. These processes can be labelled multi-photon ionisation (MPI) and collisional impact ionisation (CII) [26]. Multi-photon ionisation (MPI) occurs when multiple photons provide sufficient energy to the electrons in the valance band; as a result, the electrons are free to reach metastable quantum states by excitation. Collisional impact ionisation (CII) will take place when bound electrons gain energy from free electrons by collision; as a result, the bound electrons will be released.

As shown in **Figure 8**, when a single high fluence fs laser pulse is incident onto a material, the timescale of the physical phenomena involved in laser-material interaction can take place as follows: after 1 fs, photo-ionisation, such as multi-photon absorption and/or tunnelling ionisation, will occur; after 50 fs, avalanche ionisation will occur; and after 100 fs, thermalisation of the electrons of the metal target will take place. Longer laser pulse durations lead to more physical phenomena; after 1 ps, energy transformation from electron to lattice will result, then after 10 ps, some thermodynamic processes such as thermal diffusion, fusion and explosion will occur. In much longer laser pulses, after 1 ns, photochemical processes such as chemical reactions and phase transformation will take place [29].

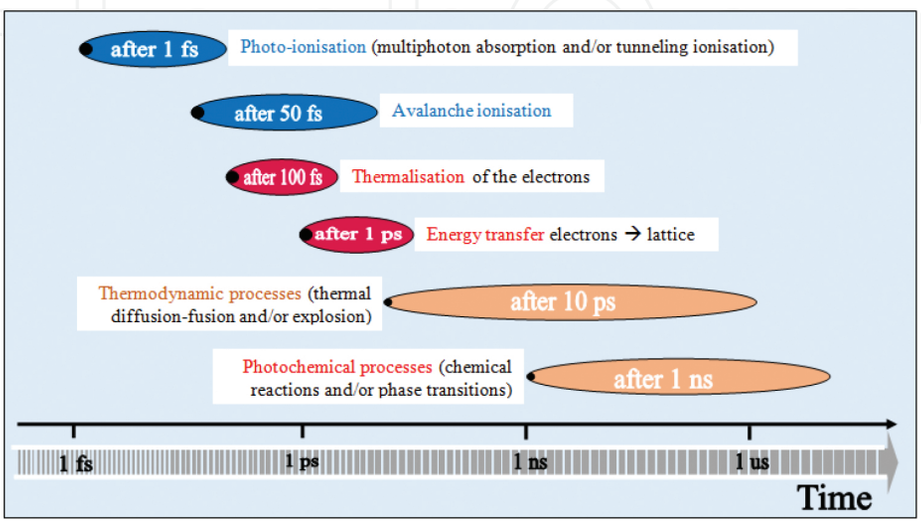

http://dx.doi.org/10.5772/63892

Figure 8. Occurrence of different physical phenomena during different timescales involved in laser-material interaction.

Different types of nanoparticles have been produced by nanosecond [30, 31], picosecond [32, 33] and femtosecond [28, 34, 35] lasers in different liquid environments, vacuum and gas media. A physical aspect of laser ablation in liquid environments is the liquid breakdown phenomena; it has been shown that the conversion efficiency of the radiation energy to a cavitation bubble during radiation focusing of different wavelengths in water is much lower for femtosecond lasers (at 100 fs, efficiency 1–2%) than for nanosecond lasers (at 76 ns, efficiency 22–25%). Femtosecond lasers (120 fs and 800 nm) can produce controllable size and size distribution of nanoparticles, while nanosecond laser produces relatively large, quite widely dispersed particles [36].

The generation of large nanoparticles in a liquid environment by nanosecond laser pulse durations and longer is due to the essential target material melting and laser pulse interaction with the cavitation bubbles that are then produced in the liquid environment [37]. The long pulse duration is sufficient to allow photon coupling with both the electronic and vibrational modes of the sample material. This case will be more predominant when the target material has low reflectivity at the laser wavelength, a large absorption coefficient, a low thermal diffusion coefficient and a low boiling point [38]. Long pulse duration heats the target material continually during the pulse duration. This causes the target material to start boiling and subsequently leads to evaporation, which produces a considerable melt layer. As a result, heat will be transferred to the target that prevents the production of very small structures and small nanoparticles. In nanosecond laser ablation, the laser power heats the target material to melting point and then vaporisation temperature; as such, this process can be considered an indirect solid-vapour transition but a solid-melt-vapour transition [19]. Nanosecond laser ablation ejects an ablation plume which creates a shielding on the surface of the material target, leading to a reduction in the laser power induced to the target. Chemistry material responses, cumulative changes in the target material's surface texture and morphology will occur due to surface melting and a combination of ablation and thermally activated processes [7].

However, the generation of small nanoparticles by short laser pulse duration is due to minimisation of both the thermal effects and the laser pulse interaction with the cavitation bubble [37]. Here, thermal conduction of the target material can be neglected because of the very short timescale and the heated area of the material being of the order of the laser absorption length α^{-1}, where α is the target material absorption coefficient [19]. At short and ultra-short laser pulse durations, because the laser interacts with materials due to very quick excitation of the electron distribution, electron-electron coupling leads to a rapid rise in the electron temperature, followed by lattice heating "at a rate dependent upon the electron-phonon coupling strength, and eventual vaporisation of the transiently heated target". Electronic contributions "can manifest themselves as unexpectedly large ion yields and/or supra-thermal propagation velocities within the expanding plasma plume" [38]. At short and ultra-short pulse durations, because the energy transfer from the electrons to the lattice happens on a longer timescale than for the short or ultra-short pulses, the pulses do not heat the target material continually. This limits the heat conduction within the target material and

produces a superheated layer the size of the irradiated volume. This leads to ablation in a specific area, resulting in minimal thermal damage. Both picosecond and femtosecond laser ablation can be viewed as a direct solid-vapour transition [19].

At short and ultra-short laser pulse durations, the ablation threshold fluence of the target materials decreases and becomes very sharply defined. In addition, the excess energy in the target still can produce thermal effects on the ablation area after the pulse has ended. Furthermore, at ultra-short laser pulse duration, the optical absorption depth reduces due to an optical breakdown caused by the ultra-short laser pulse duration; this can also cause strong absorption in otherwise transparent wide-energy band gap materials. Another advantage of picosecond and femtosecond laser ablation is that they are "separated in time from material response and ejection" [7]. In contrast, for laser production of nanoparticles in a liquid solution, the picosecond laser performs better than the femtosecond laser [37]. It can be seen that only the femtosecond laser avoided the laser-bubble interaction [22].

The size and the morphology of the nanoparticles depend on the laser pulse duration, such as whether a nano-, pico- and femtosecond laser regime is being used and the nature of the target material [39]. Hamad et al. [22] showed that the picosecond laser (10 ps and 1064 nm wavelength) produced more spherical silver nanoparticles than those produced by both nanosecond (5 ns and 532 nm wavelength) and femtosecond (100 fs and 800 nm wavelength) lasers. Under the same conditions, smaller gold nanoparticles were produced in comparison with the silver and titania, with the latter being the largest. It was also concluded that the average size of the nanoparticles was smaller for the shorter wavelength (532 nm) nanosecond laser in relation to picosecond and femtosecond lasers, showing that the role of the laser wavelength is more significant than the laser pulse duration to control the size of the nanoparticles. It is worth mentioning that some silver nanoparticles produced by nanosecond laser have irregular (non-spherical) shapes. Dudoitis et al. [40] showed that the specific nanosecond and picosecond laser parameters can be used to produce controllable particle size distribution of nickel and aluminium in argon gas.

Lescoute et al. [28] observed two groups of particles of two different sizes after femtosecond laser ablation caused by the temperature achieved in the plasma plume: these could be classified into micrometer-size fragments and nanometre-size particles for temperatures lower than the critical temperature and for higher temperatures, respectively. Kabashin and Meunier [34] used femtosecond laser ablation to produce Au nanoparticles in deionised water. The researchers observed two different groups of nanoparticles: the small (about 3–10 nm) and monodispersed particles were produced due to a mechanism which, "associated with thermal-free femtosecond ablation, manifests itself at relatively low laser fluences F, 400 J/cm^2". The second group of particles was of a larger size and a broad size distribution, produced due to plasma-induced heating and ablation that occurs at high laser fluencies. Itina [41] showed that the ultra-short laser pulses produce small nanoparticles and a stable size distribution at optimal experimental parameters. This is because while using short and ultra-short laser pulse duration, laser radiation will not be absorbed by created plasma plume. This leads to transfer much more energy into the target material during very short time. Finally, the target ejected the cluster precursors directly to the liquid solution and the plasma plume is confined to a

http://dx.doi.org/10.5772/63892

smaller volume. Chakravarty et al. [42] concluded that the smaller size of silver and copper nanoparticles can be produced by ultra-short laser pulse duration in comparison with the subnanosecond laser pulse duration. It was shown that broader surface plasmon resonance (SPR) and smaller reflection/transmission of silver and copper nanoparticles deposited by femtosecond laser in comparison with those deposited by subnanosecond laser indicating smaller size particle generation by ultra-short pulse durations. In contrast, Hubenthal et al. [43] concluded that the tailoring the size and shape of nanoparticles with nanosecond pulsed laser is more achieved in comparison with both continuous wave (CW) and femtosecond pulsed lasers.

5. Conclusions

Pulsed laser ablation for material processing and production of nanoparticles in liquid environments have been used due to the unique properties of the laser beam in marking and machining materials. There is a lack of knowledge of the optimal laser beam parameters in this field, as different laser pulse durations respond differently to different materials. A critical comparison of different laser pulse durations in micro- and nanomaterial processing was therefore sought in order to obtain higher quality and productivity. Femtosecond and picosecond lasers were found to be superior to the nanosecond laser for precision material processing. In addition, in spite of the short and ultra-short duration of their laser pulses, these lasers were observed to be more effective for the production of nanoparticles than those with longer pulse durations. Finally, laser wavelength was found to play significant role in the production of nanoparticles. The advantages of femtosecond laser ablation for micro- and nanotechnology are due to non-thermal interaction with solid target materials.

Author details

Abubaker Hassan Hamad*

Address all correspondence to: abubaker.hamad75@yahoo.co.uk

Laser Processing Research Centre, School of Mechanical, Aerospace and Civil Engineering, The University of Manchester, Manchester, UK

References

[1] Le Harzic, R., D. Breitling, M. Weikert, S. Sommer, C. Föhl, S. Valette, C. Donnet, E. Audouard and F. Dausinger, *Pulse width and energy influence on laser micromachining of*

metals in a range of 100 fs to 5 ps. Applied Surface Science, 2005. 249(1): pp. 322–331. doi:10.1016/j.apsusc.2004.12.027

[2] Rehbock, C., J. Jakobi, L. Gamrad, S. van der Meer, D. Tiedemann, U. Taylor, W. Kues, D. Rath and S. Barcikowski, *Current state of laser synthesis of metal and alloy nanoparticles as ligand-free reference materials for nano-toxicological assays*. Beilstein Journal of Nanotechnology, 2014. 5(1): pp. 1523–1541. doi:10.3762/bjnano.5.165

[3] Jaeggi, B., B. Neuenschwander, M. Schmid, M. Muralt, J. Zuercher and U. Hunziker, *Influence of the pulse duration in the ps-regime on the ablation efficiency of metals*. Physics Procedia, 2011. 12: pp. 164–171. doi:10.1016/j.phpro.2011.03.118

[4] Lucas, L. and J. Zhang, *Femtosecond laser micromachining: a back-to-basics primer*. 2012, http://www.industrial-lasers.com/

[5] Chichkov, B.N., C. Momma, S. Nolte, F. von Alvensleben and A. Tünnermann, *Femtosecond, picosecond and nanosecond laser ablation of solids*. Applied Physics A, 1996. 63(2): pp. 109–115. doi:10.1007/bf01567637

[6] Momma, C., B.N. Chichkov, S. Nolte, F. von Alvensleben, A. Tünnermann, H. Welling and B. Wellegehausen, *Short-pulse laser ablation of solid targets*. Optics Communications, 1996. 129(1): pp. 134–142. doi:10.1016/0030-4018(96)00250-7

[7] Brown, M.S. and C.B. Arnold, *Fundamentals of laser–material interaction and application to multiscale surface modification*, in *Laser Precision Microfabrication*. 2010, Springer. pp. 91–120. doi:10.1007/978-3-642-10523-4__4

[8] Han, J. and Y. Li, *Interaction Between Pulsed Laser and Materials*. Lasers-Applications in Science and Industry, K. Jakubczak, Ed. InTech, 2011. doi:10.5772/25061

[9] Sukhov, I.A., G.A. Shafeev, V.V. Voronov, M. Sygletou, E. Stratakis and C. Fotakis, *Generation of nanoparticles of bronze and brass by laser ablation in liquid*. Applied Surface Science, 2014. 302(0): pp. 79–82. doi:10.1016/j.apsusc.2013.12.018

[10] Tyurnina, A.E., V.Y. Shur, R.V. Kozin, D.K. Kuznetsov and E.A. Mingaliev, *Synthesis of stable silver colloids by laser ablation in water*. Proceedings of SPIE 2013. 9065: p. 8. doi: 10.1117/12.2053557

[11] Yan, Z. and D.B. Chrisey, *Pulsed laser ablation in liquid for micro-/nanostructure generation*. Journal of Photochemistry and Photobiology C: Photochemistry Reviews, 2012. 13(3): pp. 204–223. doi:10.1016/j.jphotochemrev.2012.04.004

[12] Amans, D., C. Malaterre, M. Diouf, C. Mancini, F. Chaput, G. Ledoux, G. Breton, Y. Guillin, C. Dujardin and K. Masenelli-Varlot, *Synthesis of oxide nanoparticles by pulsed laser ablation in liquids containing a complexing molecule: impact on size distributions and prepared phases*. The Journal of Physical Chemistry C, 2011. 115(12): pp. 5131–5139. doi:10.1021/jp109387e

[13] Amendola, V. and M. Meneghetti, *Laser ablation synthesis in solution and size manipulation of noble metal nanoparticles*. Physical Chemistry Chemical Physics, 2009. 11(20): pp. 3805–3821. doi:10.1039/B900654K

[14] Wang, X., D.M. Riffe, Y.-S. Lee and M. Downer, *Time-resolved electron-temperature measurement in a highly excited gold target using femtosecond thermionic emission*. Physical Review B, 1994. 50(11): p. 8016. doi:10.1103/PhysRevB.50.8016

[15] Schoenlein, R., W. Lin, J. Fujimoto and G. Eesley, *Femtosecond studies of nonequilibrium electronic processes in metals*. Physical Review Letters, 1987. 58(16): p. 1680. doi:10.1103/PhysRevLett.58.1680

[16] Zimmer, K., *Analytical solution of the laser-induced temperature distribution across internal material interfaces*. International Journal of Heat and Mass Transfer, 2009. 52(1): pp. 497–503. doi:10.1016/j.ijheatmasstransfer.2008.03.034

[17] Fujimoto, J., J. Liu, E. Ippen and N. Bloembergen, *Femtosecond laser interaction with metallic tungsten and nonequilibrium electron and lattice temperatures*. Physical Review Letters, 1984. 53(19): p. 1837. doi:10.1103/PhysRevLett.53.1837

[18] Stafe, M., A. Marcu and N. Puscas, *Pulsed Laser Ablation of Solids: Basics, Theory and Applications*. Vol. 53. 2013: Springer Science & Business Media. doi: 10.1007/978-3-642-40978-3

[19] Amoruso, S., R. Bruzzese, N. Spinelli and R. Velotta, *Characterization of laser-ablation plasmas*. Journal of Physics B: Atomic, Molecular and Optical Physics, 1999. 32(14): p. R131. doi:10.1088/0953-4075/32/14/201

[20] Fann, W., R. Storz, H. Tom and J. Bokor, *Electron thermalization in gold*. Physical Review B, 1992. 46(20): p. 13592. doi:10.1103/PhysRevB.46.13592

[21] Izawa, Y., Y. Setuhara, M. Hashida, M. Fujita and Y. Izawa, *Ablation and amorphization of crystalline Si by femtosecond and picosecond laser irradiation*. Japanese Journal of Applied Physics, 2006. 45(7R): p. 5791. doi:10.1143/JJAP.45.5791

[22] Hamad, A., L. Li and Z. Liu, *A comparison of the characteristics of nanosecond, picosecond and femtosecond lasers generated Ag, TiO_2 and Au nanoparticles in deionised water*. Applied Physics A, 2015. 120(4): pp. 1247–1260. doi:10.1007/s00339-015-9326-6

[23] Le Harzic, R., N. Huot, E. Audouard, C. Jonin, P. Laporte, S. Valette, A. Fraczkiewicz and R. Fortunier, *Comparison of heat-affected zones due to nanosecond and femtosecond laser pulses using transmission electronic microscopy*. Applied Physics Letters, 2002. 80(21): pp. 3886–3888. doi:10.1063/1.1481195

[24] Hirayama, Y. and M. Obara. *Molecular dynamics simulation of heat-affected zone of copper metal ablated with femtosecond laser*. in *Lasers and Applications in Science and Engineering*. 2005: International Society for Optics and Photonics. doi:10.1117/12.589513

[25] Musaev, O., A. Midgley, J. Wrobel and M. Kruger, *Laser ablation of alumina in water*. Chemical Physics Letters, 2010. 487(1): pp. 81–83. doi:10.1016/j.cplett.2010.01.011

[26] LaHaye, N.L., S.S. Harilal, P.K. Diwakar and A. Hassanein, *The effect of laser pulse duration on ICP-MS signal intensity, elemental fractionation, and detection limits in fs-LA-ICP-MS*. Journal of Analytical Atomic Spectrometry, 2013. 28(11): pp. 1781–1787. doi: 10.1039/c3ja50200g

[27] *Machining with Long Pulse Lasers, Machining with Ultrafast Laser Pulses*. 2011 [cited 2016; Available from: http://www.cmxr.com/Education/Short.html, http://www.cmxr.com/Education/Long.html

[28] Lescoute, E., L. Hallo, D. Hébert, B. Chimier, B. Etchessahar, V. Tikhonchuk, J.-M. Chevalier and P. Combis, *Experimental observations and modeling of nanoparticle formation in laser-produced expanding plasma*. Physics of Plasmas (1994–present), 2008. 15(6): p. 063507. doi:10.1063/1.2936267

[29] Royon, A., Y. Petit, G. Papon, M. Richardson and L. Canioni, *Femtosecond laser induced photochemistry in materials tailored with photosensitive agents [Invited]*. Optical Materials Express, 2011. 1(5): pp. 866–882. doi:10.1364/OME.1.000866

[30] Damian, V., C. Udrea, M. Bojan, C. Luculescu, A. Armaselu and I. Apostol. *Aluminum nanoparticles production by laser ablation in liquids*. in *International Conference on Applications of Optics and Photonics*. 2011: International Society for Optics and Photonics. doi:10.1117/12.894525

[31] Gondal, M., T.F. Qahtan, M. Dastageer, T.A. Saleh and Y.W. Maganda. *Synthesis and characterization of copper oxides nanoparticles via pulsed laser ablation in liquid*. in *10th International Conference on High Capacity Optical Networks and Enabling Technologies (HONET-CNS)*. 2013: IEEE. doi:10.1109/HONET.2013.6729774

[32] Hamad, A., L. Li, Z. Liu, X.L. Zhong and T. Wang, *Picosecond laser generation of Ag–TiO_2 nanoparticles with reduced energy gap by ablation in ice water and their antibacterial activities*. Applied Physics A, 2015. 119(4): pp. 1387–1396. doi:10.1007/s00339-015-9111-6

[33] Giorgetti, E., A. Giusti, S. Laza, P. Marsili and F. Giammanco, *Production of colloidal gold nanoparticles by picosecond laser ablation in liquids*. Physica Status Solidi (a), 2007. 204(6): pp. 1693–1698. doi:10.1002/pssa.200675320

[34] Kabashin, A.V. and M. Meunier, *Synthesis of colloidal nanoparticles during femtosecond laser ablation of gold in water*. Journal of Applied Physics, 2003. 94(12): pp. 7941–7943.

[35] Torres-Mendieta, R., R. Mondragón, E. Juliá, O. Mendoza-Yero, J. Lancis and G. Mínguez-Vega, *Fabrication of high stable gold nanofluid by pulsed laser ablation in liquids*. Advanced Materials Letters, 2015. 6(12): p. 6. doi:10.5185/amlett.2015.6038

[36] Perrière, J., E. Millon and E. Fogarassy, *Recent advances in laser processing of materials*. 2006, Elsevier.

[37] Intartaglia, R., K. Bagga and F. Brandi, *Study on the productivity of silicon nanoparticles by picosecond laser ablation in water: towards gram per hour yield*. Optics Express, 2014. 22(3): pp. 3117–3127. doi:10.1364/OE.22.003117

[38] Ashfold, M.N., F. Claeyssens, G.M. Fuge and S.J. Henley, *Pulsed laser ablation and deposition of thin films*. Chemical Society Reviews, 2004. 33(1): pp. 23–31. doi:10.1039/B207644F

[39] Kuzmin, P.G., G.A. Shafeev, G. Viau, B. Warot-Fonrose, M. Barberoglou, E. Stratakis and C. Fotakis, *Porous nanoparticles of Al and Ti generated by laser ablation in liquids*. Applied Surface Science, 2012. 258(23): pp. 9283–9287. doi:10.1016/j.apsusc.2011.08.108

[40] Dudoitis, V., V. Ulevičius, G. Račiukaitis, N. Špirkauskaitė and K. Plauškaitė, *Generation of metal nanoparticles by laser ablation*. Lithuanian Journal of Physics, 2011. 51(3): pp. 248–259.

[41] Itina, T.E., *On nanoparticle formation by laser ablation in liquids*. The Journal of Physical Chemistry C, 2010. 115(12): pp. 5044–5048. doi:10.1021/jp1090944

[42] Chakravarty, U., P. Naik, C. Mukherjee, S. Kumbhare and P. Gupta, *Formation of metal nanoparticles of various sizes in plasma plumes produced by Ti: sapphire laser pulses*. Journal of Applied Physics, 2010. 108(5): p. 053107. doi:10.1063/1.3475512

[43] Hubenthal, F., M. Alschinger, M. Bauer, D.B. Sánchez, N. Borg, M. Brezeanu, R. Frese, C. Hendrich, B. Krohn and M. Aeschliman. *Irradiation of supported gold and silver nanoparticles with continuous-wave, nanosecond, and femtosecond laser light: a comparative study*. in *Microtechnologies for the New Millennium 2005*. 2005: Proceedings of SPIE 5838, Nanotechnology II. doi:10.1117/12.608560

IntechOpen